Transient Magnetic Reconnection and Unstable Shear Layers

J. U. Brackbill and D. A. Knoll

Theoretical Division, Los Alamos National Laboratory, Los Alamos, New Mexico 87545

(Received 21 April 2000)

We study three-dimensional magnetic reconnection caused by the Kelvin-Helmholtz (KH) instability and differential rotation in subsonic and sub-Alfvenic flows. The flows, which are modeled by the resistive magnetohydrodynamic equations with constant resistivity, are stable in the direction of the magnetic field but unstable perpendicular to the magnetic field. Localized transient reconnection is observed on the KH time scale, and kinetic energy increases with decreasing resistivity. As in flux-transfer events in the Earth's magnetopause boundary layer, bipolar structures in the normal flux and bidirectional jetting away from reconnection zones are observed.

DOI: 10.1103/PhysRevLett.86.2329 PACS numbers: 94.30.Va, 52.30.–q, 94.30.Di

We present results from a computational study of reconnection that is induced by the growth of the Kelvin-Helmholtz instability (KHI) in three dimensions with an initial field that is perpendicular to the flow. Our goals are to investigate magnetic reconnection in a 3D KHI including differential rotation [1], and to understand better the role of the KHI of magnetic reconnection in the dayside magnetopause of the Earth. The study is motivated by the interaction of the solar wind with the Earth's magnetosphere. There the flow geometry results in variations in the perpendicular velocity along magnetic field lines and consequent differential rotation. Our model extends Miura's perpendicular case [2] in two ways. First, our flow speeds are subsonic and sub-Alfvenic relative to the initial field. Second, we include a third dimension parallel to the initial field with a variation of vorticity in this direction. The initial velocity shear is peaked in the center of the third dimension (equator) which results in a KHI growth rate that varies in this third dimension and produces an exponential increase in differential rotation with time [1]. This configuration is significantly different from those considered in previous KHI studies of magnetic reconnection, and its evolution results in localized reconnection on the flow time scale, a result that cannot be reproduced in 2D with an oblique field [3].

There exists a large body of literature on the KHI in MHD ([2–5], for example). This literature predominantly discusses the instability in 2D for cases with high-speed flow, and the effects of differential rotation on magnetic reconnection have not been studied. It is well known that in 2D, a magnetic field perpendicular to the flow does not affect the growth of the KHI, and does not lead to reconnection. With a magnetic field parallel to the flow, the KHI can lead to enhanced reconnection, but the initial velocity shear must be super-Alfvenic (p. 511 in Ref. [6]). We present here, for the first time, a 3D model in which a weak flow shear, combined with differential rotation, results in localized reconnection, while using a constant resistivity. It is demonstrated that the reconnection occurs on a time scale faster than a tearing mode, and that over some range of resistivity the conversion of magnetic field energy to flow energy parallel to the field increases with decreasing resistivity.

There is evidence both for the occurrence of the KHI and for magnetic reconnection at the magnetopause. The tangential velocity decreases from $100\ \mathrm{km\,s^{-1}}$ in the magnetosheath to $60\ \mathrm{km\,s^{-1}}$ in the magnetosphere [7] over a distance $\approx$800–900 km [8,9], yielding an eddy turnover or growth time for the KHI, $\approx$20 s. Since the flow in the magnetosphere and magnetosheath is subsonic and sub-Alfvenic [7], the KHI is more likely to occur at low latitudes (near the equator) where the flow is perpendicular to the magnetic field. Evidence for magnetic reconnection at the magnetopause is given by ISEE satellite observations of accelerated flows, which indicate high speed jetting away from a reconnection site [9]. The most significant feature of the data is the "extremely large" speeds, which peak at $450\ \mathrm{km\,s^{-1}}$ Recently, Phan *et al.* [10] have observed bidirectional jetting in Earth's magnetopause due to magnetic reconnection.

Reconnection at the magnetopause is observed to occur episodically, and to result in localized structures called flux transfer events (FTEs) [11]. The FTEs are characterized by a bipolar pulse of the component of the magnetic field perpendicular to the magnetopause. FTEs occur predominantly when the interplanetary magnetic field (IMF) is southward [12], and the predominant helicity of FTEs in the Northern and Southern Hemispheres is opposite in sense. The average interval between FTEs is approximately 8 min [13], or many growth times for the KHI within 30° of the subsolar point. Theoretical models for FTEs are reviewed in [14].

We model resistive MHD flow by solving equations for mass continuity, Faraday's and Ampere's laws, momentum, and energy, using a particle-in-cell algorithm [15], and a Newton-Krylov solver for the implicit equations. The flow variables are ρ, the mass density, $\mathbf{B}$, the magnetic field intensity, $\mathbf{J}$, the current density, $\mathbf{v}$, the fluid velocity, I, the specific internal energy, and p, the fluid pressure. The pressure is given by an ideal gas equation

of state, $p = (\gamma - 1)\rho I$, with $\gamma = 5/3$. The condition $\nabla \cdot \mathbf{B} = 0$ is assumed as an initial condition, and maintained subsequently by projection.

The computational domain is bisected by the equator, with its longest dimension aligned with the magnetospheric magnetic field. The computational coordinate system associates x with longitude, y with latitude, and z with the magnetopause normal, $0 \le x \le L_x$, $0 \le y \le L_y$, and $0 \le z \le L_z$, with L_x:L_y:L_z = 1:4:1. Periodic boundary conditions are imposed in x and y, and $B_z = 0$ and $v_z = 0$ at $z = 0$ and $z = L_z$.

The initial conditions are in equilibrium and correspond to a current sheet of thickness l_z. Where U is any of the magnetic field, specific internal energy, or mass density, $U(z)$ is given by $U(z) = [U]\tanh(\frac{z-0.5L_z}{l_z}) + \overline{U}$, where $\overline{U} = \frac{1}{2}(U_{\text{sphere}} + U_{\text{sheath}})$, and $[U] = \frac{1}{2}(U_{\text{sphere}} - U_{\text{sheath}})$.

The initial velocity, $v_x(t = 0)$, is discontinuous across the magnetopause, and varies with y. This flow velocity does not yield a steady-state solution, so that the initial conditions will evolve, although on a longer time scale than the KHI growth time. In the magnetosheath, the velocity is given by $v_x = \frac{1}{2}v_0 \sin(k_y y)$, and the negative of this in the magnetosphere. (This variation in velocity exaggerates the variation in y relative to x and z. More realistic models of the magnetosphere would require much larger aspect ratios than the 4:1 considered here.) In the computations, length scales are scaled by L_x, velocities by v_0, and times by the fluid transit time, $\tau = L_x/v_0$. The Mach number, $M = v_0/a$, where a is the sound speed, the Alfven Mach number, $M_A = v_0/A$, where $A = B/\sqrt{\rho}$, and the plasma beta, $\beta = p/(B^2/2)$, determine the values of B, ρ, and I. The magnetic Reynolds number, $R_m = \eta/v_0 L_x$, determines the value of resistivity. The KHI is initiated by a small, incompressible perturbed velocity, with periodicity in x such that $k_x L_x = 1$ or 2.

The values used in the southward (antiparallel) and northward (parallel) IMF calculations are summarized. Note that the densities and the magnitude of the magnetic field are the same in both cases, and thus that M_A remains the same. In both cases we have $l_z = 0.1$, $v_0 = 0.5$, a magnetosheath density of 1.0, and a magnetosphere density and field (B_y) of 0.2 and 2.041, respectively. For the southward IMF we have $I = 5.0, B_y = -1.225, \beta = 4.44, a = 2.4, A = 1.225$ in the magnetosheath, and $I = 15.0, \beta = 0.96, a = 9.13, A = 4.56$ in the magnetosphere. For the northward IMF we have $I = 2.655, B_y = 1.225, \beta = 2.4, a = 1.7, A = 1.225$ in the magnetosheath, and $I = 3.28, \beta = 0.21, a = 4.27, A = 4.56$ in the magnetosphere. In these units, the initial antiparallel configuration has a tearing mode growth rate, $\gamma \approx 0.001$ [16], and a KHI growth rate, $\gamma \approx 1.0$ [6].

The first two figures give a qualitative view of the 3D simulations. Because the perpendicular flow velocity (v_x) varies along the magnetic field direction (y), the KHI grows most rapidly at $y = 2$ where the shear is maximum. In Fig. 1, density contours at $t = 2$ show a more advanced development of the KHI at $y = 2$ than elsewhere. Reconnection caused by the KHI results in changes in the magnetic field topology in the southward IMF case, $R_m^{-1} = 0.001$, as shown in the plot of selected magnetic field lines, Fig. 2. This is not a simple X point. It is a 3D structure that is highly localized. Since resistivity is constant, the localization of reconnection in the y coordinate results from the unstable flow. Initially, the bundle of magnetic field lines shown is straight. The variation with y of the initial perpendicular velocity, v_x, causes some field line bending but no other identifiable effect. However, the variation with y of the KHI growth rate, $\gamma \sim k_x v_x(y)$, is significant. It amplifies the variation in the perturbed flow so that, for example, v_z varies exponentially with y, $v_z \sim e^{k_x v_x(y)t}$. The consequent distortion of the magnetic field causes a greater amplification of the perpendicular current, J_{perp}, at the equator relative to regions at higher latitudes. Since there is resistivity, there results a parallel

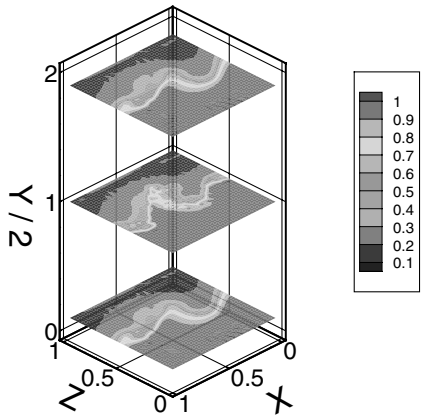

FIG. 1. Density slices show the more rapid development of the KH instability at $y/2 = 1$.

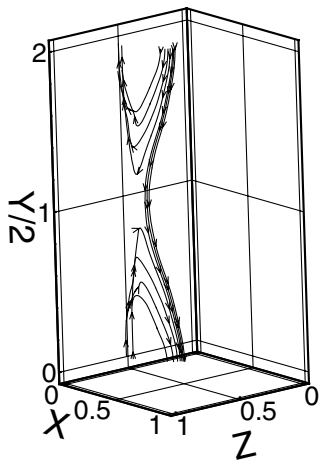

FIG. 2. Reconnected magnetic field lines are traced at $t = 3$. The reconnected lines cross the magnetopause.

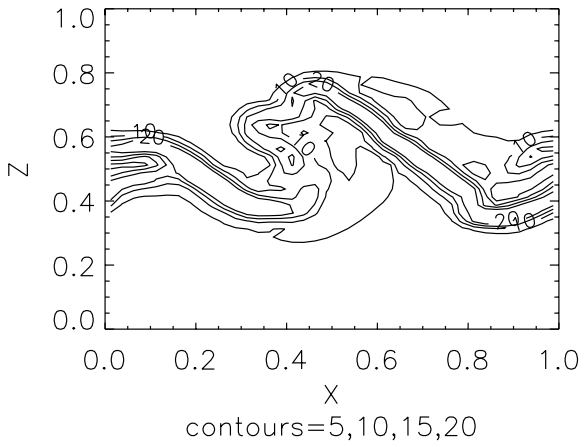

FIG. 3. Contours of the perpendicular current at $t = 3$ are plotted in the $y = 2.0$ plane.

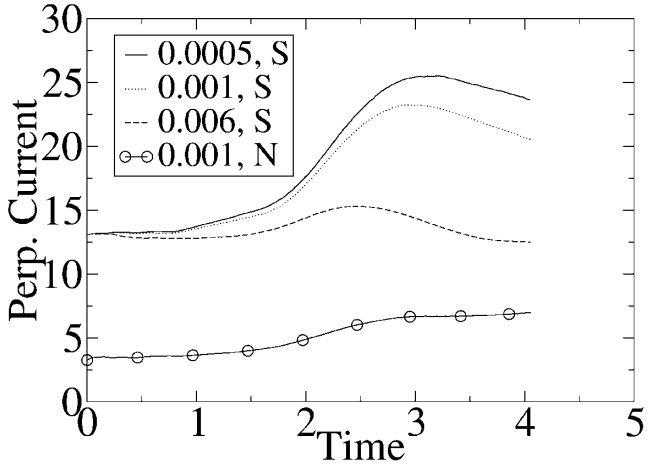

FIG. 4. Time history of the perpendicular current for various values of R_e^{-1} and southward (S) and northward (N) IMF.

gradient in the electric field ($\nabla_y E_x$) on the KHI time scale and this drives reconnection. (A localized increase in E is commonly induced by a variable resistivity with similar effect [17].)

The corresponding contours of perpendicular current density, J_{perp}, in the x-z plane at $y = 2$ are plotted in Fig. 3. The contours of J_{perp} at $t = 3$, showing current sheet folding, illustrate the amplification of the perpendicular current at the equator that is the likely cause of the reconnection shown in Fig. 2. The regions of high current are localized in the x-z plane as a result of the KH interaction. Similar current amplification is observed in two-dimensional calculations of the KHI, but with super-Alfvenic flow along the magnetic field [4]. Histories, Fig. 4, show that the total J_{perp} reaches its maximum value at $t = 3$, for $R_m^{-1} = 0.001$. When the IMF is northward, indicated by the dotted curve, J_{perp} is much smaller. When the IMF is southward, the increase in both the total, Fig. 4, and peak values of J_{perp} over their initial values are greater for smaller values of resistivity. The time scale for current amplification is the eddy turnover time.

With northward IMF, the plasma kinetic energy (all in the x direction initially) decreases with time, Fig. 5. With a southward IMF, only the mean flow in the x direction decreases. The parallel kinetic energy (y direction) increases due to reconnection. The bidirectional flow parallel to the initial magnetic field is concentrated in poleward directed jets originating at the reconnection site as observed [10]. The increase in parallel kinetic energy increases so much as the magnetic Reynolds number increases that when the inverse magnetic Reynolds number is 0.0005, the total kinetic energy increases in time. Thus, Fig. 5 indicates an increase in at least one consequence of reconnection with decreasing resistivity, opposite to the standard global tearing mode. This observation results from a competition between driven reconnection and resistive diffusion as is discussed in [18]. With lower resistivity, flow energy is converted more efficiently into magnetic field energy, which is then converted by reconnection into more parallel flow energy.

Finally we consider the relationship between these simulations and observations of FTEs for a southward IMF with $R_m^{-1} = 0.001$. Plots of the component of the magnetic field normal to the magnetopause along z, at $x = 0.5, y = 1.0$, and $y = 3.0$ from the magnetosheath to the magnetosphere, are shown in Fig. 6. (Note that these plots are in regions above and below the reconnection region.) One can see a positive-negative variation in B_z that is very much like the bipolar signatures observed in an FTE (p. 226 in Ref. [11]). The apparent helicity is induced by differential rotation, with normal sense in the Northern Hemisphere, $y > 2$, and reversed sense in the Southern Hemisphere, $y < 2$, as is observed [8]. A similar characteristic variation in B_z is observed when the variation in x is plotted at $z = 0.5, y = 1.0$, and $y = 3.0$. The variation in the normal component of the magnetic field is similar whether

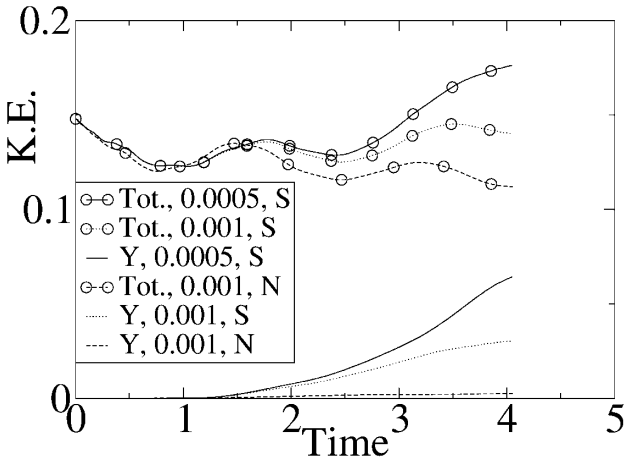

FIG. 5. Time history of the total and Y-directed kinetic energy.

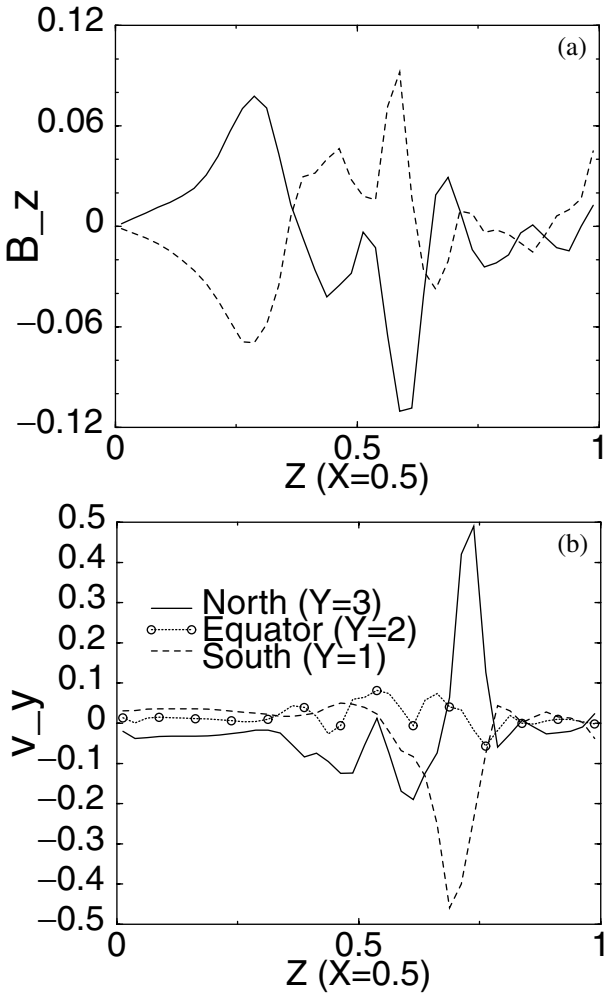

FIG. 6. The variation of the magnetopause normal component of the magnetic field with z and bipolar jetting.

one crosses or skims the magnetopause. Also plotted in Fig. 6 is v_y as one crosses the magnetopause. We see our model has reproduced the bidirectional jetting in v_y, positive in the north, negative in the south, and nonexistent at the equator, recently reported in [10]. We note that the peak values of v_y in Fig. 6 are equal to the initial values of v_x, 0.5, which is somewhat less than the observed maximum values [9].

Here we have presented the results of MHD modeling in a simple three-dimensional geometry. The flow conditions are chosen to be consistent with the low-speed nature of the real flow at Earth's magnetopause, and result in a KH instability whose strength varies along the magnetic field, thus producing differential rotation. As is shown, the unstable flow causes transient, localized reconnection, even with constant resistivity. Even though the variation in the flow velocity along magnetic field lines is exaggerated in our model problem, we argue the amplification of this variation by the KHI makes this mechanism relevant to the magnetopause. Localized, accelerated flows out of the reconnection region are observed (bidirectional jetting). Among the features of the solutions that correspond to observations of FTE's are the characteristic positive-negative variation of the magnetopause normal field as one traverses the reconnected flux, and the reversal of polarity as one crosses from the Northern to the Southern Hemisphere. The geometry of the reconnected field suggests that FTE's are generated in pairs with opposite helicities. Other results are that field-aligned currents are produced, and that the maximum perpendicular current, the conversion of magnetic field energy, and the kinetic energy of the accelerated flow increase with increasing magnetic Reynolds number.

This research is supported by the Department of Energy under Contract No. W-7405-ENG-36, and NASA Office of Space Science, Sun-Earth Connection Theory Program.

[1] H. K. Moffat, *Magnetic Field Generation in Electrically Conducting Fluids* (Cambridge University Press, Cambridge, U.K., 1978).
[2] Akira Miura, Phys. Rev. Lett. **49**, 779–782 (1982).
[3] T. W. Jones *et al.,* Astrophys. J. **482**, 230–244 (1997).
[4] C. C. Wu, J. Geophys. Res. **91**, 3042 (1986).
[5] Z. X. Liu and Y. D. Hu, Geophys. Res. Lett. **15**, 752 (1988).
[6] S. Chandrasekhar, *Hydrodynamic and Hydromagnetic Stability* (Oxford University Press, Oxford, 1961).
[7] T. D. Phan and G. Paschmann, J. Geophys. Res. **101**, 7801–7815 (1996).
[8] T. Russell, in *Magnetic Reconnection in Space and Laboratory Plasmas,* edited by E. W. Hones (American Geophysical Union, Washington, DC, 1984), pp. 124–138.
[9] G. Paschmann *et al.,* Nature (London) **282**, 243–246 (1979).
[10] T. D. Phan *et al.,* Nature (London) **404**, 848–850 (2000).
[11] R. C. Elphic, in *Geophysical Monograph* (American Geophysical Union, Washington, DC, 1995), Vol. 90, pp. 225–233.
[12] C. T. Russell, G. Le, and H. Kuo, Adv. Space Res. **18**, 197–205 (1996).
[13] H. Kuo, C. T. Russell, and G. Le, J. Geophys. Res. **100**, 3513–3519 (1995).
[14] M. Scholer, in *Physics of the Magnetosphere* (American Geophysical Union, Washington, DC, 1995), Vol. 90, pp. 235–245.
[15] J. U. Brackbill, J. Comput. Phys. **96**, 163–192 (1991).
[16] Harold P. Furth, John Killeen, and Marshall N. Rosenbluth, Phys. Fluids **4**, 459–484 (1963).
[17] T. Sato and T. Hayashi, Phys. Fluids **22**, 1189–1202 (1979).
[18] D. Biskamp, Phys. Fluids **29**, 1520–1531 (1986).